Astaxanthin-based polymers as new antimicrobial compounds

S. Weintraub [a], T. Shpigel [a], L. G. Harris [b], R. Schuster [c], E. C. Lewis [c] and D. Y. Lewitus* [a]

[a] Plastics and Polymer Engineering Department, Shenkar – Engineering Art Design, 12 Anne Frank St., Ramat-Gan, Israel 5252526

[b] Microbiology and Infectious Diseases, Institute of Life Science, Swansea University Medical School, Swansea, SA2 8PP, UK

[c] Department of Clinical Biochemistry and Pharmacology, Faculty of Health Sciences, Ben-Gurion University of the Negev, Beer-Sheva, Israel

Corresponding author: lewitus@shenkar.ac.il

Abstract

A library of novel high molecular weight polymers based on the natural carotenoid astaxanthin (ATX) has been successfully synthesized. ATX is a powerful antioxidant, known for its various therapeutic properties including anti-inflammatory and antimicrobial activities. It is a xanthophyll with a symmetric chemical structure bearing two hydroxyl groups. Thus, its copolymerization with various diacids resulted in "polyactive" polyesters with varying chemico-physio-mechanico properties (e.g., Storage moduli range: 125-1300 MPa and wetting angles of 40-110°). The potential of pATX as an antimicrobial agent was demonstrated in vitro against clinically relevant bacteria (*Staphylococcus aureus* MRSA252 and MSSA476; *S. epidermidis* 1457) showing significant reduction of both bacterial growth and biofilm formation. Lastly, we establish using pATX films in vivo had no adverse effect in direct contact with open wounds, or on the complete physiological process of whole animal wound healing.

Introduction

Few polymeric systems are based on monomers that are both naturally occurring and are inherently therapeutic. Though polymers derived from natural metabolites such as lactic acid,[1,2] or amino acids such as tyrosine[3-6] are well established in the field of implantable medical devices, these materials are designed to be benign at best with regards to any tissue interactions. Therapeutic polymers, or "polyactives", are polymer systems in which a pharmacological molecule is incorporated onto the polymer chain either as an attached pendant group, or as a structural part of the formed polymer backbone. This allows for a localized and sustained bioactive release with negligible systemic exposure.[7] In a pendant chain model, the polymer backbone generally acts as carrier, and does not

participate directly as a therapeutic entity.[8] When the bioactive molecule is a monomeric constituent of the polymer backbone, a biocompatible, biologically inert co-monomer (linker) is usually required.[7,8] Examples of the latter include various types of therapeutic inclusions, including anti-inflammatory drugs such as salicylic acid (aspirin)-derived poly(anhydride-esters),[9,10] antioxidants, antiseptics, antibiotics and analgesics.[7] Curcumin-derived biodegradable polymers are a unique example of a polyactive where the polymer backbone is made from curcumin units.[11,12] Astaxanthin (3,3'-dihydroxy-β,βcarotene-4,4'-dione) is a common nutritional, organic red pigment (Figure 1). ATX possess the empiric formula of (C40H52O4) and is produced by microorganisms such as fungi and algae, and is also found in marine animals (e.g. salmon, crustaceans) providing them with their distinct reddish colour.[13,14]

ATX has been extensively researched in the medical field due to its potent bioactivity. Recent findings include therapeutic properties, anticancer, antidiabetic, and anti-inflammatory activities, gastro-, hepato-, neuro- and cardiovascular protective effects, as well as other activities.[13,14] Moreover, ATX has been shown in various assays to significantly inhibit the growth of both Gram-positive and negative pathogens.[15,16] Despite the potential and promising applications of ATX in human health and nutrition, little effort has been directed towards using it as a polymeric prodrug. Currently, the only existing evidence is the recently described synthesis of low to medium molecular weight poly(lactides) where ATX was used as a bifunctional initiator in the ring opening polymerization process.[17] Since ATX is a highly lipophilic, low molecular weight compound,[18,19] chemical modifications through its available free hydroxyl groups improve its parenteral viability.19,20 Cardax™ is a synthetically sourced ATX modified with disodium disuccinate,[19,20] or with the amino acid lysine[21,22] to increase water solubility while maintaining therapeutic efficacy. In this work, we synthesized a library of new polymeric biomaterials based on ATX as a monomeric constituent – polyastaxanthins (pATX). These novel polymers have wide-ranging physical properties due to the use of varying dicarboxylic acid co-monomer. We subsequently established that pATXs have significant antimicrobial activity against the clinically-associated infectious pathogens *Staphylococcus epidermidis* 1457, methicillin susceptible *Staphylococcus aureus* MSSA476 and the methicillin resistant *S. aureus* MRSA252.[23] *In vivo* compliance was tested using a mouse dorsal wound model, in which the polymer was placed in direct contact with open wounds and was found to allow the unfolding of a normal process of wound healing without adverse effects. These results demonstrate the potential of pATX as a safe clinically-relevant antimicrobial agent.

Experimental

Materials and general methods

The HPLC grade organic solvents and compounds were purchased from Sigma-Aldrich Chemicals (Rehovot, Israel). Astaxanthin (ATX), was purchased from 3B Pharmachem International Ltd. (China). NMR spectra were recorded on a Varian NMRS 300 or 500 MHz instrument. 1H NMR chemical shifts are reported in ppm relative to the solvent's residual 1H signal. 13C NMR spectra were recorded at 125 MHz. Chemical shifts were expressed in δ (ppm) and coupling constants (J) in hertz units. Mn, Mw and polydispersity (Mw/Mn) were determent using Size exclusion chromatography (SEC) analysis in THF on a VE 7510, GPC (Malvern, Viscotek) at 35°C. Polymers were dissolved in THF (5mg/ml) for 24 h and the results are reported relative to polystyrene standards. Glass transition temperature (Tg) and storage moduli (E') were determined on solvent cast films using a dynamic mechanical analysis (DMA) and a TA Q800 DMA operated at -30°C to 120°C at a heating rate of 5°C min-1 using a 1 Hz frequency. The static contact angle was measured according to the sessile drop method using a contact angle analyzer (OCA 20, Dataphysics Instruments, Germany). Contact angles were measured using 5 µL water drops of deionized and ultra-filtered water (0.2 µm filter). The contact angle was measured using a video-based software (SCA 20, Dataphysics Instruments GmbH, Germany). Results are expressed as the mean of four measurements with a standard error of mean.

Polyastaxanthin synthesis

The different polymers were synthesized in a 50 ml amber scintillation vial under inert environment.1.67 mmol different diacid derivatives, 0.837 mmol DPTS, and 1.67 mmol ATX were dissolved in 8 ml dry DCM. Then, 5.026 mmol DIC was added dropwise over a 3 h period. The reaction was stirred for 24 h at room temperature. Reaction solution was then precipitated in IPA and the precipitated product was collected and dried for 30 min followed by second precipitation in EtOH then collected and vacuum-dried till further use.

Polymer film preparation

Solvent cast films of the polymer were prepared by dissolving the dried polymer in THF anhydrous (10% w/v). After complete dissolution, they were cast into a PTFE mold in a chemical hood for solvent evaporation then placed under vacuum for complete solvent evaporation. [6]

Antibacterial assays

***In vitro* toxicity evaluation**

Experiment was done in a direct contact model. L6 skeletal myocytes were grown and differentiated to myotubes cells in α-MEM medium supplemented with 2% (v/v) FCS. The cells were seeded in

triplicates in 6 well plates. Polymer films (poly(ATX-co-dodecanedioic acid); poly(ATX-co-poly(ethylene glycol) bis(carboxymethyl) ether), Avg. Mn 250 and poly(ATX-co-malonic acid)) weighing approximately 50 mg were first washed in ethanol for sterilization, then washed twice with growing medium and placed in the wells. Cells were incubated for 48 h with the different polymers. Glucose oxidase (GO) was used as a negative control (100 mU/ml of GO) added 1.15h before the termination of the experiment. Upon completion of incubation, a standard MTT test was performed.[24]

pATX-coated microtitre plates

96-well polypropylene plates were coated by dispensing 150 µl of polymeric solution (10% w/v in THF) into the wells.[25] The plates were left in the dark and the solvent was evaporated at room temperature in a fume hood. The following pATX and controls were used as coatings – ATX monomer; poly(ATX-co-sebacic acid); poly(ATX-co-hexadeceandioic acid); poly(ATX-co-poly(ethylene glycol) bis(carboxymethyl) ether), Avg. Mn 250; poly(ATX-co-poly(ethylene glycol) bis(carboxymethyl) ether), Avg. Mn 2000; poly(ATX-co-dodecanedioic acid); poly(ATX-co-pimelic acid); poly(ATX-co-malonic acid); Sebacic acid (SA); poly(ethylene glycol) bis(carboxymethyl) ether Avg. Mn 250 (PEG 250). Each compound coated 3 wells per 2 rows and the last 2 rows were left blank as control.

Bacterial strains

Staphylococcus aureus MRSA252, *S. aureus* MSSA476 and *S. epidermidis* 1457 were streaked from frozen stocks onto Columbia agar supplemented with 5 % horse blood (Oxoid, Thermo Fisher Scientific, Loughborough, UK), then incubated overnight at 37°C and used in subsequent experiments.

Bacterial growth and biofilm analysis

To determine the effect of the pATX-coatings on *S. aureus* and *S. epidermidis* growth and biofilm formation the previously described semi-quantitative adherence assay [26,27] was used and modified as follows. 3 ml Trypticase Soy Broth (TSB; Becton Dickinson, Cockeysville, USA) was inoculated with a colony from an overnight plate. Pre-cultures were grown at 37°C with shaking to mid-exponential phase (2-3 h), and then used to inoculate fresh TSB to a starting OD_{600} of 0.01 (approx. 10^5 CFU/ml). 200 µl aliquots of the suspension were then inoculated into the coated test wells (6 wells per compound) and control wells (uncoated) of the 96 well plate. The plate was then incubated in a FLUOstar OPTIMA microplate reader (BMG, Offenburg, Germany) at 37°C, and the optical density of

each well was measured at 600 nm every hour over a 24 h period. Inhibition of growth by the pATX-removed and washed with phosphate buffered saline, pH 7.4 (PBS) and air dried. All plates were stained with 150 µl crystal violet solution (Sigma-Aldrich, Gillingham, UK) for 10 min and then excess solution washed off with water. The plate was then left to air-dry before the bound, crystal violet was solubilized by addition of 95 % ethanol at 150 µl. Optical density was measured as absorbance at 570 nm using a FLUOstar OPTIMA microplate reader and biofilm positive was defined as OD_{570} above 0.2.27 All *S. aureus* and *S. epidermidis* isolates were tested in triplicate in four independent experiments. Each microtitre plate also consisted of negative controls (wells without bacterial inoculation). Data was analyzed using unpaired t-tests or one-way ANOVA, and the level of significance set at $p < 0.05$.

Animals

Female C57BL/6 mice (6-8 weeks old) were purchased from Harlan, Israel. Animal experiments were approved by Institutional Animal Care and Use Committee (BGU).

In vivo evaluation using wound closure model

In vivo dorsal wound mouse model was performed as described previously.[28] Briefly, C57BL/6 mice were anesthetized using ketamine/xylazine. Fur was removed using an electric razor and spine midline was marked with a surgical pen. Dorsal skin was folded and raised to form a 2-layer skin fold. With the animal in a lateral position, a 5-mm sterile biopsy punch was applied to remove a uniform section out of the two layers, thus forming two symmetrical full-thickness excisional wounds. Each polymer-dressed wound was therefore accompanied by its adjacent control untreated wound in the same animal. Polymer disks were soaked in sterile PBS solution 30 min prior to application to assure proper adherence to the wound. Wounds were then wrapped in sterile gauze for 48 h and presence of polymer disks was visually confirmed at the time of bandage removal. Wound area was photographed at 48 h intervals and calculated using Fiji image software analysis. Wound closure was defined as wound area < 5 % of day-0 area.

Results and discussion

Synthesis and chemical/physical characterization of p(ATX)

As demonstrated by Stupp *et al*.[29], carbodiimide-mediated coupling of diols and diacids is an efficient method for the synthesis of polyesters under mild conditions. The application of Stupp's technique towards high molecular weight polyesters with varying properties have been previously demonstrated on tyrosine derived polyarylates.[30,3] Using this method, a library of pATX polymers

were synthesized (Scheme 1) and resulted with a high molecular weight bioactive polymers with good yields. As shown in Table 1, a variety of poly(ATX)'s were synthesized using this methodology with high yield (70-95%), and as measured using GPC high molecular weight (up to 130 kDa), and relatively low polydispersity (1.2-1.9). Low PDI values in carbodiimide-mediated step growth polymerizations have been reported.[31] The effect of hydrophobic diacids lengths on the physical properties of each polymer as shown through the listed glass transition temperature (Tg) and storage moduli (Table 1) were measured using DMA. Wetting angle measurements (mean of four measurements ± SD) indicated that these polymers were hydrophobic (Table 1). Optimization of the synthesis process was conducted to determine required time and type of catalyst that would in an efficient process.[29] We compared between DMAP, the known catalyst for this kind of esterification[32] and DPTS, the catalyst used by Stupp *et al*. [29] As shown in Figure S1, the use of DPTS during 24 h resulted in superior higher Mw. We then built our library of polymers by reacting ATX with differentalkylic diacids (Scheme 1). Polyethylene glycol (PEG) was used as the hydrophilic diacids co-monomer, and was used tosynthesized a small library of p(ATX) with different Mw of PEG as co-monomer. The Mw of the PEG used ranged from 250 to 2000 (Scheme 2).The synthesis process of the PEG-based polymers was the same as with the hydrophobic diacids. Changes in the Mw of the PEG block used resulted in changes in the physical properties of the polymers, as depicted by the changes in the glass transition temperature (Tg) and storage moduli (Table 2). As expected, the wetting angle results indicate that the polymers were hydrophilic. In accordance with work by Bourke SL and Kohn J,[3] a range of properties can be reached as function of the diacid used. We observed mechanical properties that span from elastomer-like properties (highly PEGylated polymers), to stiff polymers (high alkane chains, or low PEGylation), to brittle materials (low alkane chains). Curcumin, in similarity to ATX, is a naturally occurring antioxidant, which can be applied as a diol-monomer in the synthesis of condensation polymers. Also, as pATX, curcumin-derived polymers exhibited varying physical properties with substantial bioactivity, specifically as anti-cancerous agents.[11-12,33] All chemical structures were analysed by 1H NMR, 13C NMR and two-dimensional (2D) NMR spectroscopy, which provided detailed information about the unique structure of each polymer (supp. material). NMR spectra analysis of Poly(ATX-co-dodecanedioic acid) (Figure S10) is an example for the unique structure of these polymers. Two repeating units are supposed to exist in the polymers, one is the ATX and the other is the diacid derivative. The peaks at δ 1.94-2.13 ppm were assigned to hydrogen atoms 1,34 (CH2-group) in the ATX unit while those in the diacid derivative unit at δ 2.43, 1.69, 1.24-1.41 ppm were assigned to hydrogen atoms (47,56), (48, 55), (49-51) respectively.

The peaks at δ 5.53 ppm were assigned to hydrogen atoms 2,35 (CH-group) in the ATX unit and the peaks at δ 6.05-6.74 ppm were assigned to hydrogen atoms 12,13,15,17,18,20,22,23,24,26,27,28,30,31 (CH-group) at the ATX's polyene fragment. The peaks at δ 1.22, 1.24-1.41 ppm were assigned to hydrogen atoms 7,8,41,42 (CH3-group) in the ATX unit. The peaks at δ 1.90 ppm were assigned to hydrogen atoms 9,38 (CH3-group) in the ATX unit and the peaks at δ 1.94-2.13 ppm were assigned to hydrogen atoms 16,21,44,45 (CH3-group) in the ATX's polyene fragment unit. The peaks in the 13C NMR spectrum of Poly(ATX-co-dodecanedioic acid) were also divided to the ATX unit and to the diacid unit. During the structure analysis we followed mainly after significant carbons in the ATX unit such as 2,35 and their peak at δ 70.97 ppm, carbons 3,36 and their peaks at δ 194.25 ppm and carbons 1,34 and their peaks at δ 42.70 ppm. In the diacid unit we followed mainly after carbons 40,57 and their peak at δ 173.29 ppm. The chemical shift of these carbons points on the formation of the ester bond. All other carbons were found and their chemical shifts were adjusted to their place in the repeating units (Figure S10). These results have been validated with 2D NMR spectroscopy such as COSY and HSQC (supp. Info.).

Biological activity

Antibacterial activity

Synthesis of antimicrobial polymers have been describes by Carbone-Howell et al.,[34] where inherently antimicrobial essential oils were synthesized into biodegradable poly(anhydride-esters). The hydrolysed polymer products exhibited antimicrobial activity against gram negative and gram positive bacteria. Our main aim was to synthesize ATX as polymeric antibacterial agents. A preliminary in vitro toxicity experiment was conducted using L6 cells to evaluate the impact of three polymers. We used in this assay two hydrophobic polymers that differ in their length of the co-monomers: poly(ATX-co-dodecanedioic acid); poly(ATX-co-malonic acid) and one hydrophilic polymer: Poly(ATX-co-PEG250). The results show a mild toxicity (more than 70% cell survival) after incubation for 48 h (Figure S2). Results indicated that after 48 h, more than 70% of the cells survived. In our effort to make pATX more water soluble and by doing so the polymers will be more potent, we used different PEGs as co-monomers. PEG is widely used in biomaterial synthesis, as it is known to reduce protein adsorption on polymers surfaces and increase polymer biodegradation rates.[35-37] To determine the antimicrobial properties of p(ATX), in vitro growth assays were conducted using the clinically relevant bacteria *S. epidermidis* 1457, *S. aureus* MSSA476 and *S. aureus* MRSA252, and 96 well-plates coated with different polymers with varying structures (hydrophilic and hydrophobic). Due to the complexity of this assay, we chose only four different polymers that represent the edges of each group-hydrophobic and hydrophilic. Figure 2 depicts bacterial average growth rate at the

24th hour for each polymer over no pATX control. As shown, poly(ATX-co-PEG2000), poly(ATX-co-malonic acid), Poly(ATX-co-dodecanedioic acid) and Poly(ATX-co-PEG250) were significantly resistant against all strains ($p \leq 0.001$). Poly(ATX-co-malonic acid) and Poly(ATX-co-PEG2000) exhibited bacteriostatic effect on all staphylococcal strains tested, whilst Poly(ATX-co-PEG250) and Poly(ATX-co-dodecanedioic acid) had a bactericidal effect against the tested staphylococci. Another encouraging result from this current study was the observation that different polymers showed antibacterial activity against a methicillin-resistant S. aureus strain. With the advent of antibiotic resistant bacteria and the associated risk of critically limiting surgeries, joint replacements, organ transplantation, cancer chemotherapies and other important medical procedures, there is great motivation to develop new compounds that are active against such bacteria.

As reviewed by Ivanova *et al*., current antimicrobial surface coatings tend to exhibit signs of deficiencies such as lack in long-term antibacterial activity, insufficient concentration of released agents, *etc*..[38] Thus, the pATX tested clearly show potential as antimicrobial coatings against staphylococci and importantly MRSA. Infections are commonly associated with implantable medical devices due to the ability of bacteria such as staphylococci adhere to the implant surface, resulting in significant patient morbidity and mortality.[39] Once attached bacteria have the ability to form biofilms, which can then lead to persistent infections and resistant to conventional antimicrobial treatments.[39] The ability of the bacteria to form a biofilm in the presence of the pATX coatings was determined using a semi-quantitative biofilm assay and culturing for 24 h. As shown in Figure 3, Poly(ATX-co-PEG250), Poly(ATX-co-dodecanedioic acid) and Poly(ATX-co-PEG2000) inhibit the bacteria from forming biofilms on the surfaces in comparison to the control, while poly(ATX-co-malonic acid) had no effect on biofilm formation. The amount of biofilm formed in the control wells was significantly higher to the pATX wells ($p \leq 0.001$). To date, little is known about the mechanism for antimicrobial activity of ATX.[15,16] Figure 3 illustrates significant inhibition of bacteria growth for all the ATX-based polymers tested, yet the differences in activity between the polymers and the modus operandi are still unknown.

***In vivo* evaluation of pATX**

Importantly, such compounds must accommodate physiological processes related to the mentioned above procedures, most importantly, wound closure and tissue repair. Normal wound healing is a complex, concerted process involving parenchymal cells, extracellular matrix and soluble mediators, such as growth factors and cytokines, and is highly susceptible to local interferences. Our study directly challenged the polymers in this regard in a highly stringent model for physiological wound

healing. Disks made from different polymers were tested in vivo to determine their effect on exposure to live tissue. Uniformly generated open wounds on the dorsum of mice were directly covered in full contact with the disks, and their effect on the delicate process of normal wound healing was compared to same-animal bare wounds. As shown in Figure 4, polyastaxanthin exhibited no effect on the normal wound closure process, exhibiting a consistent colour change dynamic and no macroscopic differences in tissue appearance. As reviewed by Orgill *et al*., todays clinical wound healing implants are facing quite a few problems such as mechanical mismatch with the body and most importantly inability to postpone or eliminate infections.[40] The development of polymeric material with varying physical properties that are made from a naturally-derived monomer that is inherently antimicrobial could have with further development significant impact of such devices.

Conclusions

New astaxanthin-based bioactive polymers have been synthesized and characterized. By using different diacids as co-monomers, different physico-chemical-mechanical properties were obtained for each. The novel use of ATX as constituent in the polymer backbone has shown promising results as an antibacterial agent in vitro, specifically against MRSA. Along with its tissue-accommodating nontoxic nature, as established in the *in vivo* wound healing model, pATX has great potential as a useful material for coating of medical devices, as well as an antibacterial agent. More research is required to fully appreciate the spectrum of advantages and potential medical use of these novel polyactives.

Acknowledgements

This work was sponsored by the Israeli Ministry of Economy Innovation Authority grant # 56284, and iPROMEDAI COST (European Cooperation in Science and Technology) Action (TD1305) short-term scientific mission grant (ECOST-STSM-TD1305-170416-072287).

References

1 R. K. Kulkarni, E. G. Moore, A. F. Hegyeli, F. Leonard, J. Biomed. Mater. Res., 1971, 5, 169.

2 R. Langer, D. A. Tirrell, Nature, 2004, 428, 487.

3 S. L. Bourke, J. Kohn, Adv. Drug. Deliv. Rev., 2003, 55, 447.

4 D. Lewitus, K. L. Smith, W. Shain, J. Kohn, Acta. Biomater., 2011, 7, 2483.

5 D. Lewitus, R. J. Vogelstein, G. Zhen, Y. S. Choi, J. Kohn, S. Harshbarger, X. Jia, IEEE. Trans. Neural. Syst. Rehabil. Eng., 2011, 19, 204.

6 D. Y. Lewitus, K. L. Smith, W. Shain, D. Bolikal, J. Kohn, Biomaterials., 2011, 32, 5543.

7 N. D. Stebbins, J. J. Faig, W. Yu, R. Guliyev, K. E. Uhrich, Biomaterials. Science., 2015, 3, 1171.

8 K. Hoste, K. De Winne, E. Schacht, Int. J. Pharm., 2004, 277, 119.

9 L. Erdmann, K. E. Uhrich, Biomaterials., 2000, 21, 1941.

10 R. Jabara, N. Chronos, K. Robinson, Cathet. Cardiovasc. Intervent. 2008, 72, 186.

11 N. Shpaisman, L. Sheihet, J. Bushman, J. Winters, J. Kohn, Biomacromolecules. 2012, 13, 2279.

12 H. Tang, C. J. Murphy, B. Zhang, Y. Shen, E. A. Van Kirk, W. J. Murdoch, M. Radosz, Biomaterials. 2010, 31, 7139.

13 J. P. Yuan, J. Peng, K. Yin, J. H. Wang, Mol. Nutr. Food. Res. 2011, 55, 150.

14 R. R. Ambati, S. M. Phang, S. Ravi, R. G. Aswathanarayana, Mar. Drugs., 2014, 12, 128.

15 U. N. Ushakumari, R. Ramanujan, Int. J. Pharm., 2013, 2, 67.

16 A. Mageswari, P. Subramanian, R. Srinivasan, S. Karthikeyan, K. M. Gothandam, Microbiol. Res., 2015, 179, 38.

17 H. Middleton, S. Tempelaar, D. M. Haddletona, A. P. Dove, Polym. Chem., 2011, 2, 595.

18 M. Háda, V. Nagy, J. Deli, A. Agócs, Molecules, 2012, 17, 5003.

19 S. F. Lockwood, G. J. Gross, Cardiovasc. Drug. Rev., 2005, 23, 199.

20 D. A. Frey, E. W. Kataisto, J. L. Ekmanis, S. O'Malley, S. F. Lockwood, Org. Proc. Res. Dev. 2004, 8, 796.

21 S. N. Naess, H. R. Sliwka, V. Partali, T. B. Melø, N. K. Razi, H. L. Jackson, S. F. Lockwood, Chem. Phys. Lipids. 2007, 148, 63.

22 H. L. Jackson, A. J. Cardounel, J. L. Zweier, S. F. Lockwood, Bioorg. Med. Chem. Lett. 2004, 14, 3985.

23 U. Römling, C. Balsalobre, J. Intern. Med., 2012, 272, 541.

24 T. Getter, I. Zaks, Y. Barhum, T. Ben-Zur, S. Böselt, S. Gregoire, O. Viskind, T. Shani, H. Gottlieb, O. Green, M. Shubely, H. Senderowitz, A. Israelson, I. Kwon, S. Petri, D. Offen, A. Gruzman, ChemMedChem. 2015 ,10, 850.

25 P. M. Kou, N. Pallassana, R. Bowden, B. Cunningham, A. Joy, J. Kohn, J. E. Babensee, Biomaterials, 2012, 33, 1699.

26 D. Mack, N. Siemssen, R. Laufs, Infect. Immun., 1992, 60, 2048.

27 L. G. Harris, A. Bexfield, Y. Nigam, H. Rohde, N. A. Ratcliffe, D. Mack, Int. J. Artif. Organs., 2009, 32, 555.

28 C. F. Moreira, P. Cassini-Vieira, M. F. da Silva, L. S. Barcelos, Bio-protocol, 2015, 5, e1662.

29 J. S. Moore, S. I. Stupp, Macromolecules, 1990, 23, 65.

30 S. Brocchini, K. James, V. Tangpasuthadol, J. Kohn, J. Am. Chem. Soc., 1997, 119, 4553.

31 S. Gokhale, Y. Xu, A. Joy, Biomacromolecules, 2013, 14, 2489.

32 B. Neises, W. Steglich, Angew. Chem, 1978, 90, 554; B. Neises, W. Steglich, Angew. Chem. Int. Ed. Engl, 1978, 17, 522.

33 N. Matsumi, N. Nakamura, K. Aoi, Polymer Journal, 2008, 40, 400.

34 A. L. Carbone-Howell, N. D. Stebbins, K. E. Uhrich, Biomacromolecules, 2014, 15, 1889.

35 N. Weber, H. P. Wendel, J. Kohn, J. Biomed. Mater. Res. A., 2005, 72, 420.

36 P. A. Johnson, A. Luk, A. Demtchouk, H. Patel, H. J. Sung, M. D. Treiser, S. Gordonov, L. Sheihet, D. Bolikal, J. Kohn, P. V. Moghe, J. Biomed. Mater. Res. A., 2010, 93, 505.

37 D. Y. Lewitus, F. Rios, R. Rojas, J. Kohn, J. Mater. Sci. Mater. Med., 2013, 24, 2529.

38 J. Hasan, R. J. Crawford, E. P. Ivanova, Trends. Biotechnol., 2013, 31, 295.

39 P. M. Kou, N. Pallassana, R. Bowden, B. Cunningham, A. Joy, J. Kohn, J. E. Babensee, Biomaterials, 2012, 33, 1699.

40 T. T. Nyame, H. A. Chiang, D. P. Orgill, Surg. Clin. North. Am., 2014, 94, 839.

Figures and Tables

Table 1. Physical properties of p(ATX) Derivatives

Polymer	*Mw*(Daltons)	*Mn*(Daltons)	PDI(*Mw/Mn*)	*Tg* (°C)	Storage Modulus (MPa)	(Θ)
poly(ATX-co-malonic acid)	57,200	40,100	1.42	-	-	-
Poly(ATX-co-suberic acid)	54,500	38,800	1.40	53	1207	88.0 ± 1.7
Poly(ATX-co-Sebacic acid)	130,400	78,500	1.66	48.4	1388	96.9 ± 1.1
Poly(ATX-co-dodecanedioic acid)	114,800	64,600	1.77	39	365	109.0 ± 5.2
Poly(ATX-co-Hexadecanedioic acid)	102,500	59,500	1.72	22	125	103.9 ± 2.9

Table 2. Physical properties of poly[ATX-co-peg(biscarboxymethyl ether)] derivatives

Polymer	*Mw*(Daltons) [a]	*Mn*(Daltons) [a]	PDI(*Mw/Mn*) [a]	*Tg* (°C) [b]	Storage Modulus (MPa) [b]	(Θ)
Poly(ATX-co-PEG_{250})	88,200	45,800	1.92	44	1200	91.5 ± 3.1
Poly(ATX-co-PEG_{600})	38,000	18,800	2.02	5.67	-	67.3 ± 1.3
Poly(ATX-co-PEG_{2000})	59,700	15,000	3.98	-36.93	125	46.15 ± 7.1

a) Mn, Mw and polydispersities (Mw/Mn) were determined by GPC. b) Tg (°C) and Storage Modulus (MPa) were determinate by DMA.

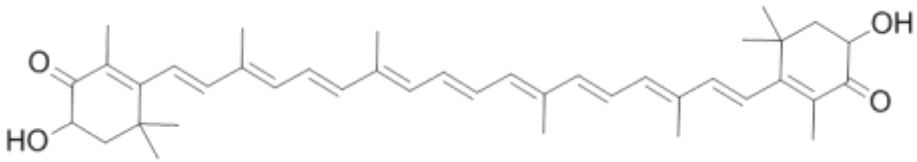

Figure 1. Astaxanthin structure

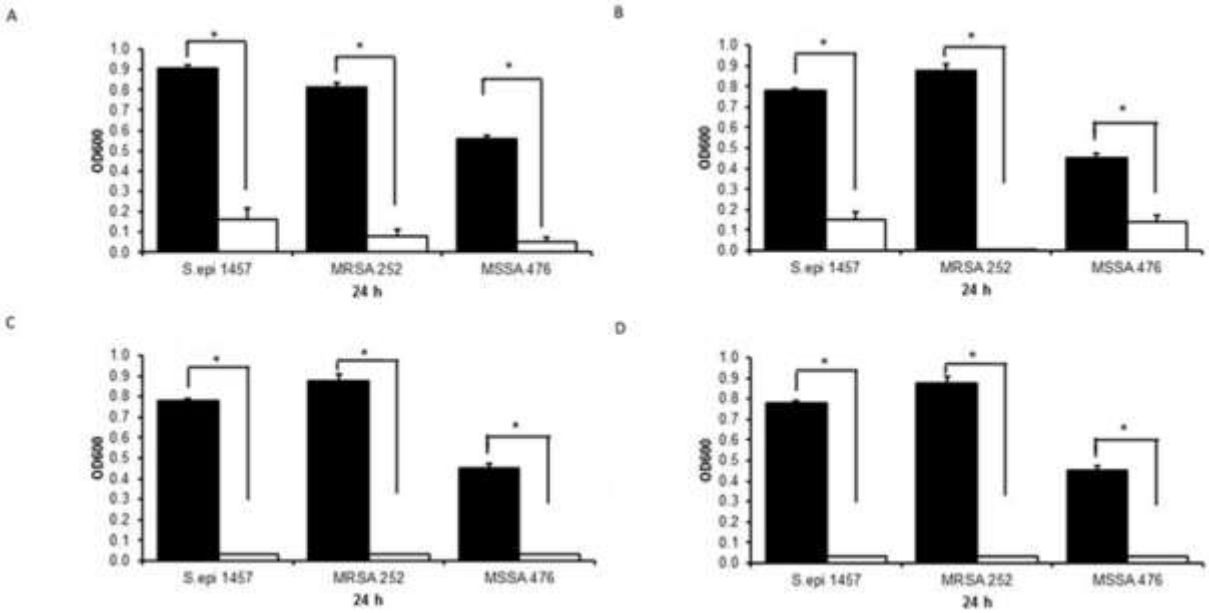

Figure 2. Effect of pATX coatings on the average growth at 24h of *S. epidermidis* 1457, *S. aureus* MRSA252 and *S. aureus* MSSA476 isolates grown on (A) poly(ATX-co-malonic acid), (B) Poly(ATX-co-PEG2000), (C) Poly(ATX-co-PEG250) and (D) Poly(ATX-co-dodecanedioic acid). Control black and pATX coating white; mean±SEM, * $p \leq 0.001$. The effect of pATX copolymers on the growth of *S. epidermidis* 1457, S. aureus MRSA252 and S. aureus MSSA476 during a whole 24 h period is shown in Figure S11.

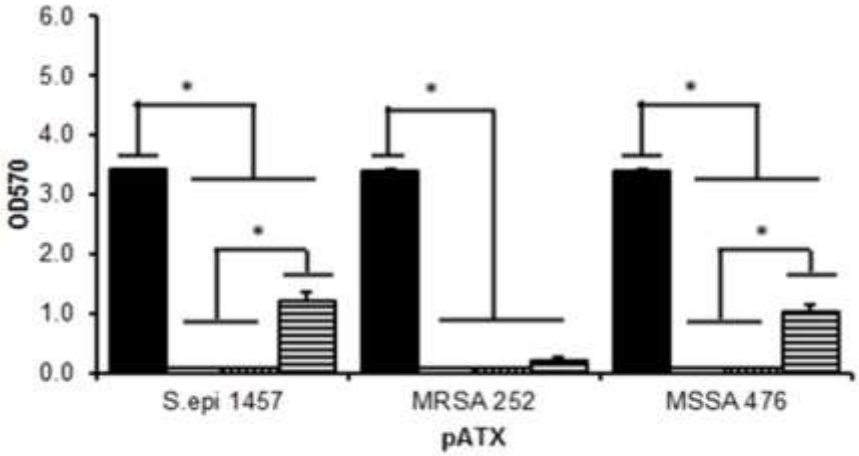

Figure 3. Biofilm formation of *S. epidermidis* 1457, *S. aureus* MRSA252 and *S. aureus* MSSA476 on the different pATX surfaces. Black-control, white - Poly(ATX-co-PEG250), diagonal lines - Poly(ATX-co-dodecanedioic acid) and stripes - Poly(ATX-co-PEG2000). Mean ± SEM, * $p \leq 0.001$.

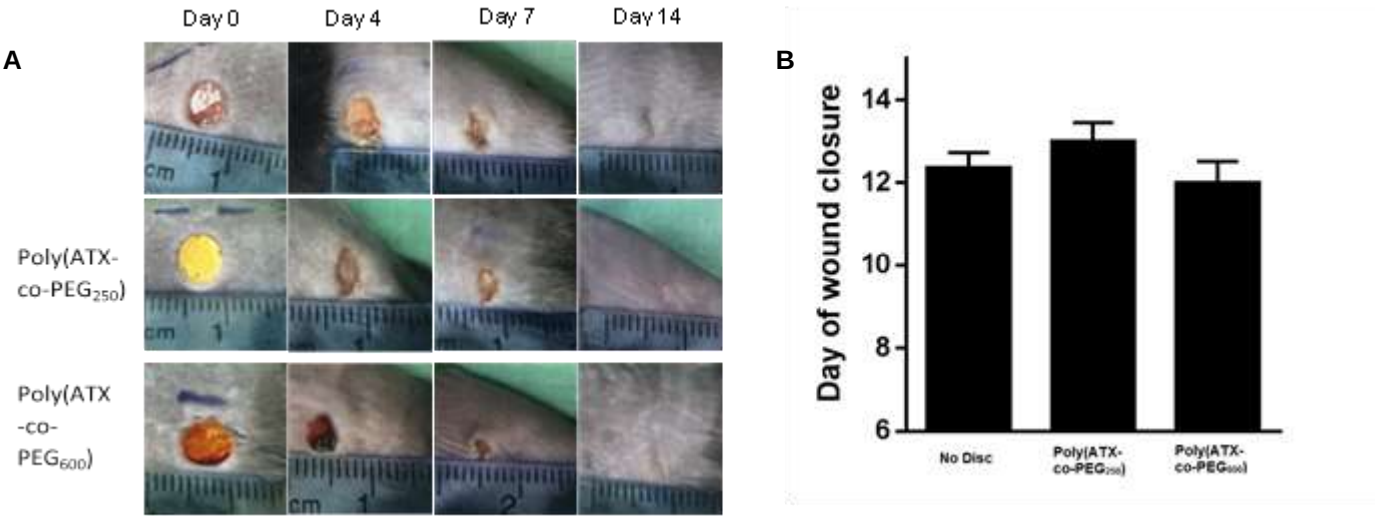

Figure 4. Results demonstrating the effect of pATX polymers in the *in vivo* wound closure study. (A) Representative images at indicated time-points and (B) Pooled data from 2 separate experiments; wound closure defined as wound area <5% of day-0 area. Mean±SEM.

Scheme 1. Synthesis of p(ATX) with different alkyl diacids

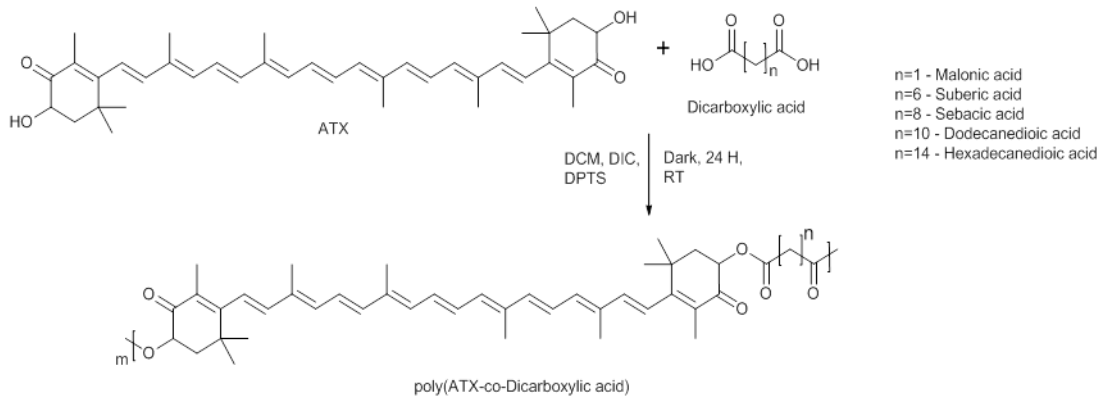

Scheme 2. Synthesis of p(ATX) with different PEG